Available online at www.sciencedirect.com
ScienceDirect
The Veterinary Journal 174 (2007) 435–438
The Veterinary Journal
www.elsevier.com/locate/tvjl

Short Communication

Comparison of computed tomographic images of normal cranial and upper cervical lymph nodes with corresponding E12 plastinated-embedded sections in the dog

S. Kneissl [a,*], A. Probst [b]

[a] Department for Diagnostic Imaging, Infectious Diseases and Clinical Pathology, University of Veterinary Medicine, Vienna, Austria
[b] Department of Pathobiology, University of Veterinary Medicine, Vienna, Austria

Accepted 15 September 2006

Abstract

To document normal lymph nodes on computed tomographic images, 102 scans were reviewed of dogs that had computed tomography (CT) of the head and upper cervical region. If lymph nodes were identified, symmetry, density, homogeneity, and size, as well as the relation to the surrounding fat tissue were noted. CT images with distinct asymmetric, enlarged, and obliterated lymph nodes were excluded. To improve the detailed anatomical topography, corresponding E12 plastinated-embedded sections of a dog were used. Compared with muscle tissue, normal lymph nodes were slightly hypodense and had a homogeneous parenchyma. Mandibular and retropharyngeal lymphocentres could be seen consistently and CT proved to be a useful method both to detect their presence and to assess their morphology. It was not possible to identify the parotid lymph node consistently because of the lack of tissue contrast at the lymph node–gland interface.

Keywords: CT; Lymph nodes; Head; Dog

Staging of tumours allows reasonable predictions to be made that will guide clinical and owner decisions. Assessment of metastasis to regional lymph nodes is of major importance in determining treatment and ultimate survival. Canine primary brain neoplasms, such as gliomas and meningiomas, are usually solitary. However multiple primary brain tumours and extracranial metastasis of primary brain meningioma have been reported (Moore et al., 1996; Schulman et al., 1992).

The most frequently seen secondary neoplasms of dogs include nasal adenocarcinoma, pituitary adenoma or carcinoma, and cranial metastasis from mammary, prostatic, pulmonary adenocarcinoma or haemangiosarcoma (Kornegay, 1986; Patnaik et al., 1986). Local infiltration, cerebrospinal fluid seeding and haematogenous metastases are the major patterns of spread of canine brain tumours. As treatment of primary brain tumours become widespread, the subject of tumour spread will become more important. It is likely that an increase in various patterns of spread, including spread via lymphatics, will be evident in association with the increased life expectancy that accompanies the successful therapy of dogs with a primary brain tumour (LeCouteur, 2001).

Up to now, imaging of cranial and upper cervical lymph nodes by means of computed tomography (CT) has been limited in dogs (Fike et al., 1980; George and Smallwood, 1992; Probst et al., 1996; Zook et al., 1981). In particular, studies dealing with cranial neoplasia did not analyze information regarding the regional lymph nodes that would have been vital in assessing malignancy (Cherubini et al., 2005; Hathcock and Newton, 2000). Hence, the purpose of this retrospective study was to document topography and morphology of normal cranial and upper cervical lymph nodes on canine CT images.

* Corresponding author. Tel.: +43 1 250775464; fax: +43 1 250775790.
E-mail address: sibylle.kneissl@vu-wien.ac.at (S. Kneissl).

1090-0233/$ - see front matter
doi:10.1016/j.tvjl.2006.09.005

We reviewed 102 CT scans (CT Pace, General Electric) undertaken in the Department of Diagnostic Imaging, Infectious Diseases and Laboratory Medicine, Clinic of Diagnostic Imaging, University of Veterinary Medicine, Vienna. The dogs, which were of various breeds, ages and gender, had undergone CT of the head and upper cervical region during 2005. For all animals, CT scans consisted of a plain series, as well as a contrast series, after an intravenous (IV) administration of contrast medium (Scanlux, Sanochemia AG) at a dose of 740 mg/kg body weight. The technical settings were 80–120 kV and 120–160 mAs. The matrix was 512 × 512 cm, and the field of view was 6.5–8.6 cm. Slice thickness and distance were 2–3 mm.

The scans were evaluated retrospectively in a soft tissue window (WL 90, WW ± 350). If lymph nodes were identified, symmetry, homogeneity, density and size, as well as their relation to the surrounding fat tissue, were recorded. Diameters were recorded in millimetres, and were not related to the size of the animal (Table 1). CT images with distinct alterations of the lymph nodes were excluded. To improve the detailed anatomical topography, the corresponding E12 plastinated-embedded sections of a middle-sized dog were used. The transverse slices had a thickness of approximately 2 mm.

Table 1
CT landmarks, size, number of nodes and detections rate of cranial and upper cervical lymph nodes

Lymphocenter	Landmark	Length (mm)	Number of lymph nodes (Detection rate %)
Mandibular	Facial vein	10–25	3–4 (100%)
Parotid	Temporomandibular joint, parotid gland	n.a.	1–2 (14%)
Medial retropharyngeal	Mandibular gland, common carotid artery	30–70	1 (100%)

n.a., Not accessed.

Compared with muscle tissue (56.6 ± 5.8 HU), normal lymph nodes were slightly hypodense (36.6 ± 13.3 HU) and had a similar homogeneous parenchyma. After IV contrast application, they enhanced homogeneously and were then hyperdense (110.3 ± 3.3 HU) compared with the muscular tissue (66 ± 4.6 HU). In some cases, a hypodense, triangular lymph node area, the presumed hilus, indented the capsule.

Three or four circular to ovoid mandibular lymph nodes were seen consistently along both sides of the facial vein. This lymphocentrum contrasted well with the surrounding fatty tissue. The length of a single lymph node varied from 10 to 25 mm (Fig. 1).

The parotid lymph node could not be identified consistently, since it was difficult to differentiate from the surrounding isodense parotid gland parenchyma (plain study: 38.3 ± 6.0 HU; contrast study: 80.8 ± 3.6 HU). Also, the corresponding E12 plastic-embedded sections did not improve the topography. As a result, we refrained from potentially inaccurate diameter measurements (Fig. 2).

The medial retropharyngeal lymph node was positioned within a fatty, triangular space, defined by the wing of the atlas dorsomedially, the mandibular gland ventrolaterally, and the common carotid artery medially. The isodense mandibular gland (plain study: 45.0 ± 6.0 HU; contrast study: 114.6 ± 5.3 HU) was a consistent landmark to localize this lymph node at its caudomedial aspect. In all cases, the normal lymph node had the shape of an irregular to bilaterally flattened structure. The diameter (length × height × width) of the medial retropharyngeal lymph node was approximately 30–70 × 10 × 5–10 mm (Fig. 3).

CT and magnetic resonance imaging (MRI) have proved to be invaluable tools for evaluating the soft tissue structures of the neck. Although there are many imaging modalities available for the evaluation of a neck mass, including radiography and ultrasonography, CT and MRI provide detailed anatomical location in relationship

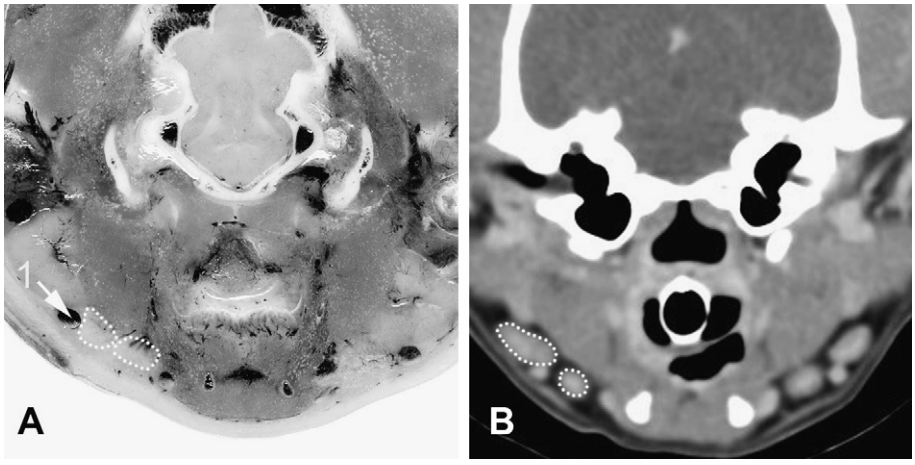

Fig. 1. Transverse, plastinated-embedded (A) and post-contrast, CT cross-section (B) displayed in a soft tissue window (WL 90, WW ±350), at the level of the mandibular lymph nodes (. . .) (1) facial vein.